Astronomy & Astrophysics manuscript no. main
September 5, 2014

Nickel mass estimates of Type Ia Supernovae from NIR data: Test case for SN2014J and SN2006X

TBD

[1] European Southern Observatory, Karl Schwarzschild Strasse 2, Garching bei Munchen, Germany, 85748
e-mail: @eso.org
[2]

Preprint online version: September 5, 2014

Abstract

Aims. To determine the relation between the amount of Nickel produced in SNIa and the timing of the second maximum and to extrapolate Nickel mass values for highly reddened SNIa using this relation
Methods. We measure the (pseudo)-bolometric luminosity at peak and use it to derive a value of M_{Ni} mass for a 'low-reddening' sample of objects from the literature in order to minimize effects from presuming a reddening law.
Results. We find a strong correlation between the M_{Ni} and t_2 in the Y and J bands and a weaker trend in the H band. We use this empirical relation to derive M_{Ni} for test case SN with high extinction. This allows us to have a M_{Ni} value which is independent of the reddening law applied. We also apply the relation to all objects not in the low-reddening sample for which a t_2 is measured.
Conclusions. From our results we conclude that an empirical relation between M_{Ni} and t_2 can allow us to infer the M_{Ni} for highly reddened objects without an estimate of their total absorption. The results for SN2014J from this method correspond well with the values obtained from recent γ ray observations, thus providing further evidence of the potency of this technique

Key words. stars: supernovae: general

1. Introduction

Type Ia supernovae (SNe Ia) have been used as cosmological distance indicators and have provided first evidence for the accelerated expansion of the universe (Riess et al. 1998; Perlmutter et al. 1999). . Their potency as cosmological probes has led to dedicated efforts to understand the nature of these explosions to reduce effects from systematics in the constraints of the cosmological parameters.

SNIa in the optical, however, require corrections using correlations between observables (Phillips 1993; Tripp 1998) to improve cosmological parameter estimation. Recent studies of SNeIa have indicated that the SNIa are much more uniform in the NIR, which has led to systematic efforts in obtaining NIR light curves of Ia's. Another interesting feature of SNIa in the NIR is a second maximum that appears $\sim$ 15-35 days after maximum light in B-band. Kasen (2006) demonstrated that the second maximum could be the result of decrease in opacity due to the ionization change of Fe group elements from doubly to singly ionized atoms, which preferentially radiate the energy at near-IR wavelengths. He further indicated that larger iron mass would lead to a later maximum in the NIR light curves. Recent studies have shown a strong dependence of the timing of the second maximum (hereafter t_2) on the decline rate of the SNIa, indicating that brighter explosions have a later onset of the second maximum. A strong relation between the t_2 and the onset of the uniform optical colour phase (hereafter t_L, see also t_{max} Burns et al. 2014) suggests that the second maximum is related to the colour evolution which is tied to the amount of iron group elements synthesized in the explosion (Kasen & Woosley (2007)).

Send offprint requests to: TBD

The conclusion from these studies point to a connection between the $M_{^{56}Ni}$ in SNIa and t_2.

In this study, we investigate ,directly, the link between the $M_{^{56}Ni}$ and t_2. We use a sample of nearby objects with low extinction from dust, in order to circumvent uncertainties from the specific reddening law used. We aim to use this relation to derive $M_{^{56}Ni}$ for heavily extinguished SNae where using the bolometric peak is extremely sensitive to the total absorption value used, and hence, the reddening law. To this end, we propose using NIR only data at late times along with an empirical relation to obtain precise estimates of $M_{^{56}Ni}$ for objects where other methods provide disparate results.

2. Data

The sample for this study is constrained by objects which have NIR observations at late times as well as well-sampled optical and NIR light curves to construct a (pseudo-) bolometric light curve. The main data source of near-infrared photometry of SNe Ia currently comes from the Carnegie Supernova Project (CSP; Contreras et al. 2010; **?**; Stritzinger et al. 2011; Phillips 2012; Burns et al. 2014). They form an ideal basis for an evaluation of light curves parameters. We add to this sample objects from the literature and the nearby objects eg. SN2011fe.

Since we aim to circumvent the uncertainties from host galaxy extinction, we only select objects with an $E(B-V)_host$ value less than 0.1. Since we want to investigate the connection of M_{Ni} with t_2 in the NIR, this excludes objects which are spectroscopically similar to the peculiar SN 1991bg (Filippenko et al. 1992; Leibundgut et al. 1993; Mazzali et al. 1997) and objects that do not exhibit a second maximum (SNe 2005bl, 2005ke,

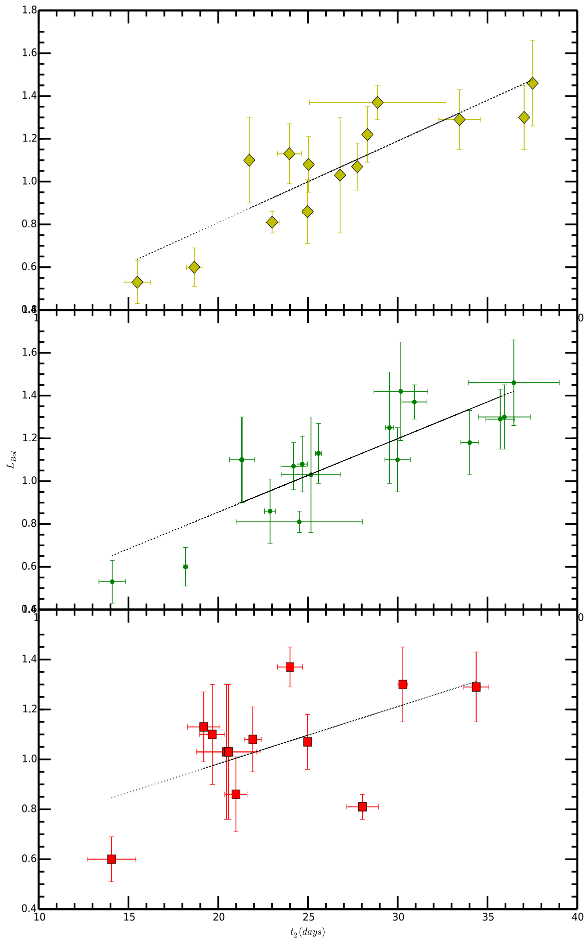

Figure 1. L_{max} is plotted against the t_2 in YJH bands. A strong correlation is observed in the Y and J, whereas a weaker correlation is seen in the H band. Best fit lines are overplotted in black**this only includes objects with a u-H measured bolometric peak and not any of the others**

2005ku, 2006bd, 2006mr, 2007N, 2007ax, SN2007ba, 2009F). On similar lines we exclude peculiar objects like 2006bt and 2006ot. These constraints leave us with a final sample of 22 objects.

3. Analysis

The flux emitted by an SNIa in the UV, optical and NIR traces the radiation converted from the radioactive decays of newly synthesized isotopes. As the SN emits most of its flux in the UV to NIR passbands, the "uvoir bolometric flux" represents a physically meaningful quantity (Suntzeff 1996)

We select a low-reddening sample so that our measurements are less sensitive to a reddening law. For objects with sufficient amount of near maximum data in the optical and the NIR, we construct UBVRIJH bolometric light curves. We do not use K band data since there are very few objects in the sample with well-sampled K band light curves. For objects with well-sampled K light curves we calculate the flux emitted in the K band and find that it is between $1-3\%$, thus, not using the K-band is not a dominant source of uncertainty. The magnitudes were corrected for reddening using a CCM reddening law for each filter. The values for the extinction are presented in table 2. The uncertainty in the reddening estimate was propagated into the calculation of the bolometric flux Using zero-points in the given filters, the magnitudes were converted to fluxes. The resulting light curve, in ergs/cm^2/s was converted into an absolute bolometric light curve by using the distances of the SN derived from the host galaxy redshift.

Since all distances are scaled to an $H_0 = 70 kms^{-1} Mpc^{-1}$the errors in the luminosity distance are only affected by the relative errors in the distance moduli (see Table 2 for values and uncertainty estimates). For objects not in the hubble flow, we use distance measurements from published estimates (which use others methods eg. Cepheid, Tully-Fisher relation etc.).

The bolometric light curves were interpolated using a cubic spline. In order to get an $L_{Bol}(max)$ we required sampling in the individual bands at pre-maximum epochs. Thus, for objects without NIR coverage before B_{max}, we use the UBVRI light curves. The errors on the peak were calculated from the errors in the fluxes of the bolometric maximum using a Monte Carlo for 1000 realisations of the light curve.

For objects with no NIR coverage near maximum, we apply a correction like in Stritzinger et al. (2006) and increase the M_{Ni} value by 1.1. In **?**, the authors found that using a UVOIR light curve with the correction for the NIR, Arnett's rule estimates the M_{Ni} to $\leq 0.05\ M_{\odot}$.

Table 3. Values of the coefficients for correlations between L_{max} and t_2 in the individual filters

Filter	a_i	b_i
Y	0.040(±0.005)	-0.055(±0.125)
J	0.042(±0.004)	-0.039(±0.102)
H	0.033(±0.000)	-0.239(±0.203)

4. Results

In this section we present the results derived from the measurements of the peak bolometric luminosity and the trends observed with other observables for the SNe in our low-reddening sample, as well as the complete sample of objects with a measured timing of the second maximum

4.1. Correlation between L_{max} and t_2

In figure 1, we find that there is a very strong correlation between t_2 and M_{Ni} in the Y and J bands with r values of 0.80, 0.88. A much weaker trend is observed in the H band with $r\sim 0.60$. This is reflected in the ratio of the slope to the slope error in equation (**??**) In the Y and J band, a strong correlation suggests that objects with more Ni produced show later second maxima.

$$L_{max} = a_i \cdot t_2(i) + b_i \tag{1}$$

From Table 3, we can see that the constraints on the slope for the best fit relation in the H band are weak. Hence, for further analyses, we do not use the H band. Equations (**??**) relate the timing of the second maximum to the peak bolometric luminosity by combining equation (3) with equation (**??**). We can see

Table 1. The sample of SNe which have low reddening, as defined in the text. The references for the data are presented along with the extinction values and the distanes used to calculate the bolometric light curves

SN	μ	e_μ	$E(B-V)_{host}$	$E(B-V)_{MW}$	Filters
SN2001ba	35.40	0.50	0.010(0.04)	0.021 (0.002)	UBVRIJH
SN2002dj	31.70	0.30	0.020(0.03)	0.080 (0.003)	UBVRIJH
SN2002fk	32.59	0.15	0.030(0.01)	0.030 (0.003)	UBVRIJH
SN2004gu	36.59	0.04	0.096(0.034)	0.022(0.001)	BVRI
SN2005M	35.01	0.09	0.060(0.021)	0.027(0.002)	UBVRIJH
SN2005am	32.85	0.20	0.053(0.017)	0.043(0.002)	UBVRIJH
SN2005el	34.04	0.14	0.015(0.012)	0.098 (0.001)	UBVRIJH
SN2005eq	35.46	0.07	0.044(0.024)	0.063(0.003)	UBVRIJH
SN2005hc	36.50	0.05	0.049(0.019)	0.028(0.001)	UBVRIJH
SN2005iq	35.80	0.15	0.040(0.015)	0.019(0.001)	UBVRIJH
SN2005ki	34.73	0.10	0.016(0.013)	0.027(0.001)	UBVRIJH
SN2005na	35.34	0.08	0.061(0.022)	0.068(0.003)	UBVRI
SN2006bh	33.28	0.20	0.037(0.013)	0.023(0.001)	UBVRIJH
SN2007as	34.45	0.12	0.050(0.011)	0.123(0.001)	UBVRI
SN2007bd	35.73	0.07	0.058(0.022)	0.029(0.001)	UBVRIJH
SN2007nq	36.44	0.05	0.046(0.013)	0.031(0.001)	BVRI
SN2007on	31.45	0.08	< 0.007	0.010(0.001)	UBVRIJH
SN2008R	33.73	0.16	0.009(0.013)	0.062(0.001)	UBVRIJH
SN2008bc	34.16	0.13	< 0.019	0.225(0.004)	UBVRIJH
SN2008gp	35.79	0.06	0.098(0.022)	0.104(0.005)	UBVRIJH
SN2008hv	33.84	0.15	0.074(0.023)	0.028(0.001)	UBVRIJH
SN2008ia	34.96	0.09	0.066(0.016)	0.195(0.005)	UBVRIJH
SN2011fe	28.91	0.20	0.03(0.01)	0.021(0.001)	UBVRIJH

Table 2. L_{max} measurements for low reddening SNIa with a measured t_2.

SN	$L_{max}(\cdot e^{43} ergs^{-1})$	e_L	$M_{Ni} - Arn(M_\odot)$	$M_{Ni} - Arn(M_\odot)$ (fixed rise)	$M_{Ni} - DDC(M_\odot)$
SN2001ba	1.18	0.15	0.575092	0.59000	0.56844
SN2002dj	1.25	0.26	0.592183	0.625000	0.611612
SN2002fk	1.42	0.23	0.683269	0.709999	0.755999
SN2004gu	1.3	0.15	0.661581	0.649999	0.652212
SN2005M	1.37	0.08	0.696507	0.685000	0.708912
SN2005am	1.1	0.2	0.466534	0.550000	0.524371
SN2005el	0.91	0.11	0.3978	0.455000	0.44
SN2005eq	1.32	0.2	0.667858	0.660000	0.674324
SN2005hc	1.46	0.2	0.743015	0.730000	0.790152
SN2005iq	1.07	0.11	0.480249	0.535000	0.510746
SN2005ki	1.03	0.27	0.452258	0.514999	0.490739
SN2005na	1.42	0.24	0.681671	0.709999	0.755999
SN2006bh	0.86	0.15	0.371834	0.430000	0.404027
SN2007as	0.81	0.05	0.364402	0.405000	0.382924
SN2007bd	1.22	0.13	0.5508	0.61000	0.5934
SN2007nq	0.91	0.17	0.385686	0.455000	0.431355
SN2007on	0.6	0.09	0.242248	0.300000	0.278019
SN2008R	0.53	0.1	0.206321	0.264999	0.251168
SN2008bc	1.32	0.19	0.631442	0.660000	0.674324
SN2008gp	1.29	0.14	0.621706	0.644999	0.641555
SN2008hv	1.08	0.13	0.482169	0.540000	0.517519
SN2008ia	1.13	0.14	0.498953	0.564999	0.545635
SN2011fe	1.1	0.15	0.504791	0.550000	0.524371

that the relation is dependent on the rise time of the SN and the α parameter which encodes the deviation from Arnett's rule.

From the equations it is evident that the timing of the second maximum in H doesn't provide stringent constraints on the bolometric peak luminosity.

4.2. Low galactic reddening sample

In our sample, we selected objects with a host galaxy extinction < 0.1 mag. For some of these objects, the galactic extinction is > 0.1 mag. In order to see whether these objects influence the strength of the correlation, we evaluate the correlation coefficients for a sample without the high galactic reddening objects. As a result, 7 objects with $E(B-V)_{host}$ <0.1 but total E(B-V) $\geq$ are removed. We do not find a substantial decrease in the correlation coefficients in the YJH bands, which are 0.76, 0.83, 0.60 respectively. Since we know the reddening law in the MW with high certainty, we can correct the bolometric light curves for the absorption from the MW dust. Thus, for further analysis we do not truncate the sample from the original low reddening objects in Table 1

4.3. Deriving M_{Ni} from L_{max}

In the sections above, we have found a strong correlation between the peak bolometric luminosity (L_{max}) and t_2 in the Y and J bands.

Since our final aim is to derive a value of the Nickel mass for objects which have a measured value of t_2, we present the different methods to derive M_{Ni} from the peak bolometric luminosity.

In figure 4, we plot the distributions of the M_{Ni} from the different methods.

4.3.1. Arnett's rule with a variable rise time

Arnett's rule states that the luminosity of the SN at peak is given by the instantaneous rate of energy deposition from radioactive decays inside the expanding ejecta. This is summarized in equation (**??**).

$$L_{max} = \alpha E_{Ni}(t_R) \tag{2}$$

Where E_{Ni} is the input from ^{56}Ni decay at maximum, t_R is the rise time and α accounts for deviations from Arnett's Rule.

$$E_{Ni}(1M_\odot) = 6.45 \cdot 10^{43} e^{-t_R/8.8} + 1.45 \cdot 10^{43} e^{-t_R/111.3} \tag{3}$$

For estimates using different rise times, we follow the relation in **?**

$$t_{R,B} = 17.5 - 5(\Delta m_{15} - 1.1) \tag{4}$$

and

$$t_{R,Bol} = t_{R,B} + (t_{max,bol} - t_{max,B}) \tag{5}$$

which implies

$$L_{max} = \alpha \cdot (6.45 \cdot 10^{43} e^{-(t_{R,bol}/8.8)} + 1.45 \cdot 10^{43} e^{-t_{R,bol}/111.3}) \cdot (M_{Ni}/M_\odot) \tag{6}$$

substituting the relation derived between L_{max} and t_2 (equation (1)) we get a relation between t_2 and M_{Ni}

$$M_{Ni} = \frac{a_i \cdot t_2(i) + b_i}{\alpha \cdot E_{Ni}(t_2(i))} \tag{7}$$

From equation (7), we can see that the relation between M_{Ni} and t_2 is non-linear.

4.3.2. Arnett's rule with a fixed rise time

For this method of deriving M_{Ni} from L_{max}, we use a fixed rise time of 19 days, as in **?**. Similar to their analysis, we propagate an uncertainty of $\pm$ 3 days

$$L_{max} = (2.0 \pm 0.3) \cdot 10^{43} (M_{Ni}/M_\odot) ergs^{-1} \tag{8}$$

For deriving equation (8) we need to use a specific value of α. In previous studies (eg. Stritzinger et al. 2006; Mazzali et al. 2007), authors use α=1. This value is very close to the self consisent models of Arnett (1982) and is also the mean values for the models of Höflich, Khokhlov & Wheeler (1995). Hence, in our study, we use α=1.

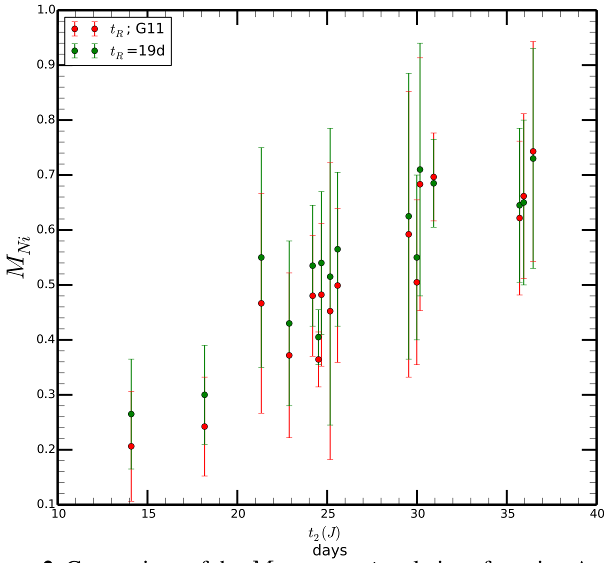

Figure 2. Comparison of the M_{Ni} versus t_2 relations for using Arnett's rule with variable (*red circles*) and fixed (*green circles*) rise time.

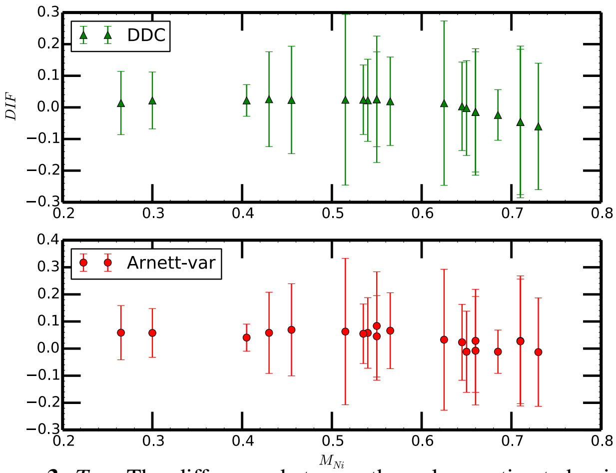

Figure 3. *Top*: The difference between the values estimated using a fixed rise time with Arnett's rule and the DDC models is plotted against the estimates from Arnett's rule with fixed rise time. *Bottom*: The difference between values estimated using a fixed rise time with Arnett's rule and a variable rise time plotted against the estimates from Arnett's rule with fixed rise time. From the two panels we can see that the difference in the individual measurements are much smaller than the errors from a given method

4.3.3. Interpolating using DDC models

From these bolometric light curves, we derive M_{Ni} values by interpolating the relation between $L_{bol}(max)$ and M_{Ni} from the DDC models of Blondin et al. (2013) For objects without NIR coverage near maximum, we interpolate the values for the synthetic pseudo-bolometric light curves calculated only using the UBVRI filters. For SN2004gu and SN2007nq, which only has near maximum coverage in the $BVRI$ filters, we use the model value for only that set of filters. This method, therefore, has the advantage of being able to derive M_{Ni} values for objects with missing passbands without an additional correction term applied to the bolometric luminosity.

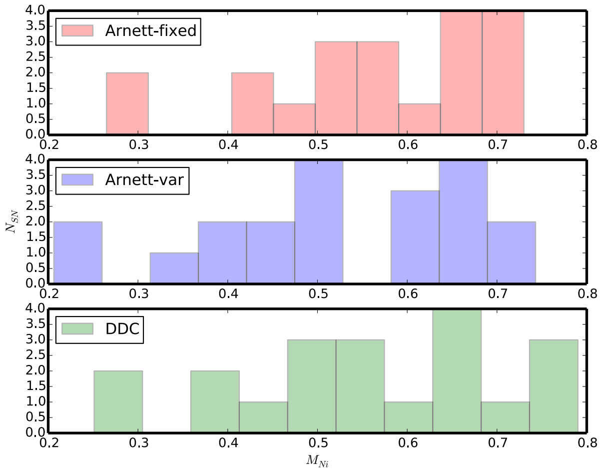

Figure 4. The histograms show the different methods to estimate the M_{Ni} from the L_{max}. The values from Arnett's rule with fixed and variable rise time are plotted in the *top* and *middle* panels. The *bottom* panel has the values estimated from the DDC models

4.4. Test Case for SN2014J and SN2006X

Using the correlations derived above, we want to estimate the Ni masses of heavily reddened SNae. The first test case is the nearby SN 2014J in M82 with an $E(B-V)_{host}$ of 1.3. Current attempts to use the bolometric light curve depend on the A_V value used and vary by a factor of ~ 2 (0.37 $M_\odot$ if using A_V=1.7 mag from Margutti et al. (2014), compared to 0.77 using a higher A_V of 2.5 mag from Goobar et al. (2014)). In our analyses the aim is to estimate the M_{Ni} independent of the extinction.

The proximity of SN2014J, has allowed for the first γ ray Co line detection in an SNIa (Churazov+ 2014). the authors, using a line photon escape fraction from the models, deduce an Ni mass of 0.62 ± 0.13 $M_\odot$. This provides a direct measurement of M_{Ni} for the SN. However, γ ray detections aren't possible for farther away SN, for which we require a different estimation method.

Using the best fit relation for the sample defined above , we obtain M_{Ni} of 0.59 ± 0.23 $M_\odot$ for a t_2 of 28.37 ± 5.7 days. Thus, we find a very good correspondence between the values from the γ rays and the NIR second maximum. This adds evidence to the argument that the NIR can be used for estimate M_{Ni} for highly reddened SN, even in more distant objects for which γ ray Co line detections are not possible This uncertainty in M_{Ni} can be reduced with a more precise estimate of t_2. For SN2014J, we can get a precise measurement of the extinction from IR spectra at $\sim$ +300 days. This is also not possible for objects farther away. Thus, we apply this relation to a farther away, heavily extinguished object, SN2006X. The measured value for SN2006X of $t_2(J)$ is 28.19 with an error of 0.49 days. This results in an M_{Ni} value of 0.57 ± 0.13 $M_\odot$. We can see that a smaller uncertainty in t_2 gives a more accurate measurement of M_{Ni}. We compare this value for SN2006X to that obtained using $t_2(Y)$ and obtain M_{Ni} of 0.58 ± 0.17 $M_\odot$. We find both these values consistent with each other. The slightly higher error bar on the value from $t_2(Y)$ is due to a larger error on the intercept in the best fit relation for the Y band.

The derived value of M_{Ni} is consistent with the conclusion that SN2006X is a 'normal' SNIa (**??**).

We include three more objects in the highly reddened sample, namely, 1986G, 2005A and 2008fp. We calculate the M_{Ni} for these objects in the same way as for SN2014J and SN2006X. We summarise our findings in Table 4.4. We can see that 1986G

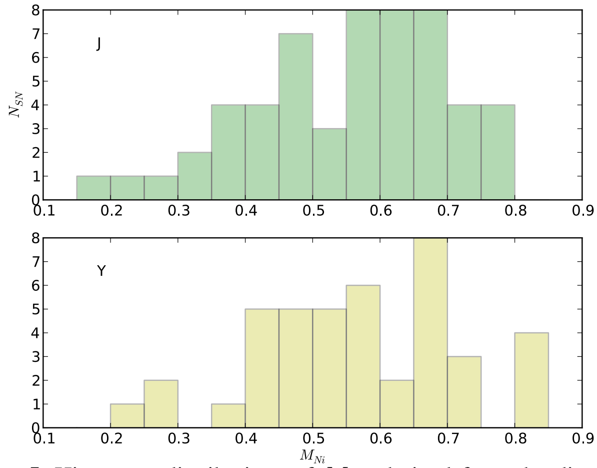

Figure 5. Histogram distributions of M_{Ni} derived from the distributions of t_2 for a complete sample of SNIa with measured t_2. This uses the Arnett's rule derivation with fixed

has a lower value of M_{Ni} than the other objects in the sample. This is consistent with the observed optical decline rate and lower B band luminosity of the SN. Since we find that t_2 in both Y and J bands correlates very strongly with the M_{Ni}, we use combined constraints from the relations to obtain an M_{Ni} estimate. We can see from Table 4.4 that the error on the M_{Ni} reduces when using combined constraints. For 2014J, it is 0.17 $M_\odot$ whereas for the others it is much lower at 0.07 $M_\odot$

Hence, we conclude that the NIR second maximum timing (in Y and J) is a very good indicator of the amount of Nickel synthesised in the explosion, even for heavily reddened objects.

4.5. Complete NIR Sample

Since we have derived the relation between L_{max} and t_2 and have presented the different ways to obtain the M_{Ni} from the L_{max}, we can then use the distribution of t_2 for all objects, independent of reddening to obtain a distribution of M_{Ni} using the relations derived The evaluated masses are summarized in Table 4.5

From figure 5, we find a large scatter in the M_{Ni} values. We find that the objects vary by a factor of 3 in their M_{Ni} distribution. We note, however, that since 91bg-like objects do not show a second maximum, we do not have values in the figure $\lesssim 0.2$ $M_\odot$

In figure 6, we plot the difference between the M_{Ni} estimated from the t_2 in Y and J bands against the M_{Ni} estimated from $t_2(J)$. We find that there is no relation between the two quantities. The mean difference is 0.03 $M_\odot$ with a standard deviation of 0.037 $M_\odot$. This is lower than the error estimate on the individual values, which is seen in the figure.

4.6. Comparison with published values

We searched the literature for published values of M_{Ni} for objects in our sample. In Scalzo et al. (2014) , the authors published values of M_{Ni} for 2005el and 2011fe. For 2011fe, we find M_{Ni} of 0.52 ± 0.15 $M_\odot$ whereas the value in S14 is 0.42 ± 0.08. We note that the value of α in their study is 1.2 whereas we use α=1. Using their value of α, we find M_{Ni}= 0.44 $M_\odot$, which is a better agreement.

For SN2005el we find M_{Ni} of 0.44 $\pm$ $M_\odot$. Scalzo et al. (2014) provides a discussion of this object, which in their sample

Table 4. Comparison of different methods to estimate M_{Ni} for SN2014J

M_{Ni} (inferred)	σ	Method	Reference
0.62	0.13	γ ray lines	Churazov 2014
0.37	–	Bolometric light curve A_V=1.7 mag	Margutti 2014
0.77	–	Bolometric light curve A_V=2.5 mag	Goobar 2014
0.58	0.17	NIR second maximum	this work

Table 5. M_{Ni} estimates for 5 objects with high values of $E(B-V)_{host}$. We present constraints from the relation using only $t_2(J)$ as well as from both $t_2(Y)$ and $t_2(J)$. We can see a marked decrease in the error values when combined constraints are used

SN	$t_2(J)$	M_{Ni} (inferred)	σ	μ	e_μ	Method
SN1986G	16.40 ($\pm$ 1.4)	0.23	0.12	28.01	0.12	J band relation
–	–	0.25	0.07	–	–	combined fit
SN2005A	27.58 ($\pm$ 0.31)	0.54	0.15	34.51	0.11	J band relation
–	–	0.56	0.07	–	–	combined fit
SN2006X	28.19 ($\pm$ 0.49)	0.57	0.13	30.91	0.08	J band relation
–	–	0.57	0.07	–	–	combined fit
SN2008fp	31.01 ($\pm$ 1.4)	0.63	0.15	31.79	0.05	J band relation
– -	–	0.65	0.07	–	–	cf
SN2014J	28.37 ($\pm$ 5.71)	0.58	0.23	27.64	0.10	J band relation
–	–	0.59	0.17	–	–	combined fit

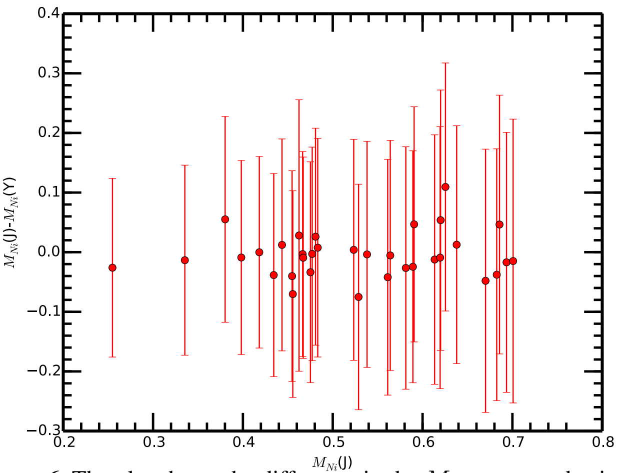

Figure 6. The plot shows the difference in the M_{Ni} measured using Y and J band data, plotted against the M_{Ni} measured from the J band data. The mean value of the difference is 0.03 $M_\odot$ with a standard deviation of 0.037 $M_\odot$ (error bars on the x-axis have not been plotted for better visibilty of points)

they measure to have an M_{Ni} of 0.52. It is one of two outliers in their M_{Ni}-Δm_{15}. They argue that it is likely for the SN to have a lower M_{Ni} that their fiducial analysis suggests.

5. Discussion and Conclusion

In our sample, we observe a strong correlation between the M_{Ni} and t_2 in Y and J, and less so in the H band. This provides us with direct evidence that the timing of the second maximum is governed by the amount of Nickel produced by the supernova since it leads to a later ionization transition of the iron group elements at late time (mainly, ^{56}Co) from doubly to singly ionized (Kasen 2006).

This relation offers great insight into measuring the M_{Ni} for objects not in the low-reddening sample, but with extensive NIR data. A striking example of this application is the nearby SN2014J in M82, which is heavily occluded by host galaxy dust. Since this prevents an accurate measurement of M_{Ni} from the bolometric light curves and there is a large disparity in the different values published in the literature using this method, we use the relations we obtain to constrain the M_{Ni}. For SN2014J, we have a unique opportunity to compare different estimation methods, since its proximity has allowed γ ray Co line detection and therefore, another extinction independent measurement of the M_{Ni}. Our value of 0.58 $\pm$ 0.21 $M_\odot$ compares very well with Churazov et al. (2014), who find M_{Ni} of 0.61 $\pm$ 0.13 $M_\odot$. The brightness of SN2014J at late times, due to its proximity, permits us to obtain NIR spectra at $\sim$ 300 days, which can provide an accurate measurement of the extinction and therefore, an accurate M_{Ni} from the bolometric light curve. This presents us with a confrontation of several different methods to measure the M_{Ni} and hence obtain a conclusive estimate on the amount of Ni produce in this SN.

The recent discovery of ^{56}Ni in the outer layers of the ejecta of SN2014J (Diehl et al. 2014) offers insight into the nature of the ejecta structure. Our analysis cannot account for the Ni in the outer layers and therefore, the total amount of Ni produced would be greater than the value of 0.58 $M_\odot$ we have obtained.

Since γ detections are unlikely for farther out SN and most of them are too faint at $\sim$ +300 days for IR spectroscopy, we apply our method to other heavily reddened SN that are farther away than SN2014J. The first object we analyse is SN2006X. From the measurement of 0.57 $\pm$ 0.15 $M_\odot$, we conclude that 2006X produced the average amount of Ni for an SNIa. We also

References

Ajhar E. A., Tonry J. L., Blakeslee J. P., Riess A. G., Schmidt B. P., 2001, ApJ, 559, 584
Amanullah R., et al., 2014, ApJ, 788, 21
Arnett W. D., 1982, ApJ, 253, 785
Barbon R., Ciatti F., Rosino L., 1973, A&A, 25, 241
Benetti S., et al., 2004, MNRAS, 348, 261
Biscardi I., et al., 2012, A&A, 537, A57
Blondin S., Dessart L., Hillier D. J., Khokhlov A. M., 2013, MNRAS, 429, 2127
Branch D., Tammann G. A., 1992, ARA&A, 30, 359
Burns C. R., et al., 2014, ApJ, 789, 32
Cardelli J. A., Clayton G. C., Mathis J. S., 1989, ApJ, 345, 245

Table 6. M_{Ni} measurements for the complete sample of objects with t_2 measurements in both Y and J bands.

SN	M^a_{Ni} (J)	σ	M^a_{Ni} (Y)	σ
2004ey	0.55972	0.18827	0.60606	0.20078
2004gs	0.41960	0.16062	0.42107	0.16925
2004gu	0.69188	0.22776	0.71609	0.22037
2005A	0.52479	0.18464	0.52129	0.18149
2005M	0.58898	0.20305	0.55098	0.24945
2005al	0.47613	0.18247	0.48234	0.17790
2005am	0.40632	0.17355	0.40616	0.16814
2005el	0.46279	0.17583	0.46756	0.18239
2005eq	0.66908	0.21120	0.72553	0.22212
2005hc	0.70353	0.24425	0.72078	0.21973
2005iq	0.45502	0.17702	0.52855	0.18467
2005ki	0.47669	0.19151	0.50547	0.17686
2005na	0.63129	0.20410	0.51847	0.19134
2006D	0.48280	0.18409	0.46976	0.17538
2006X	0.54244	0.18385	0.54012	0.18786
2006ax	0.61693	0.20145	0.62951	0.20647
2006bh	0.42938	0.17432	0.47265	0.17540
2006et	0.62377	0.21597	0.62562	0.20453
2006hb	0.38320	0.17574	0.32494	0.15151
2006kf	0.45352	0.17771	0.49185	0.19541
2007S	0.68068	0.21642	0.72577	0.23435
2007af	0.56375	0.19466	0.57156	0.19483
2007as	0.46589	0.22175	0.43634	0.17288
2007bm	0.52969	0.17733	0.60822	0.20281
2007le	0.58617	0.19980	0.60800	0.19635
2007nq	0.45044	0.18491	0.43375	0.16546
2007on	0.33502	0.15770	0.34958	0.15819
2008C	0.62455	0.21035	0.56493	0.18960
2008R	0.24824	0.14855	0.28520	0.14514
2008bc	0.64159	0.21423	0.62800	0.20448
2008fp	0.59200	0.20136	0.62030	0.20927
2008gp	0.69018	0.21778	0.63983	0.21465
2008hv	0.46871	0.17814	0.47176	0.17940
2008ia	0.48278	0.17542	0.45173	0.17370

Cartier R., et al., 2014, ApJ, 789, 89
Churazov E., et al., 2014, Natur, 512, 406
Contardo G., Leibundgut B., Vacca W. D., 2000, A&A, 359, 876
Contreras C., et al., 2010, AJ, 139, 519
Diehl R., et al., 2014, arXiv, arXiv:1407:3061
Filippenko A. V., et al., 1992, AJ, 104, 1543
Folatelli G., et al., 2010, AJ, 139, 120
Foley R., et al., 2014, arXiv, arXiv:1405.3677
Freedman W. L., et al., 2001, ApJ, 553, 47
Friedman A. S., et al., 2014, arXiv, arXiv:1408.0465
Ganeshalingam M., Li W., Filippenko A. V., 2011, MNRAS, 416, 2607
Goobar A., Leibundgut B., 2011, ARNPS, 61, 251
Goobar A., et al., 2014, ApJ, 784, L12
Hillebrandt W., Niemeyer J. C., 2000, ARA&A, 38, 191
Höflich P., Khokhlov A., Wheeler C., 1995, ASPC, 73, 441
Jack D., Hauschildt P. H., Baron E., 2012, A&A, 538, A132
Jensen J. B., Tonry J. L., Barris B. J., Thompson R. I., Liu M. C., Rieke M. J., Ajhar E. A., Blakeslee J. P., 2003, ApJ, 583, 712
Jha S., Riess A. G., Kirshner R. P., 2007, ApJ, 659, 122
Kasen D., 2006, ApJ, 649, 939
Kasen D., Woosley S. E., 2007, ApJ, 656, 661
Kattner S., et al., 2012, PASP, 124, 114
Krisciunas K., et al., 2001, AJ, 122, 1616
Krisciunas K., et al., 2003, AJ, 125, 166
Krisciunas K., et al., 2004a, AJ, 127, 1664
Krisciunas K., et al., 2004b, AJ, 128, 3034
Krisciunas K., et al., 2007, AJ, 133, 58
Krisciunas K., et al., 2009, AJ, 138, 1584
Kromer M., Sim S. A., 2009, MNRAS, 398, 1809
Leaman J., Li W., Chornock R., Filippenko A. V., 2011, MNRAS, 412, 1419
Leibundgut B., 1988, PhD thesis, University of Basel
Leibundgut B., 2000, A&ARv, 10, 179
Leibundgut B., 2001, ARA&A, 39, 67
Leibundgut B., et al., 1993, AJ, 105, 301
Leloudas G., et al., 2009, A&A, 505, 265
Li W., et al., 2001, PASP, 113, 1178
Li W., et al., 2003, PASP, 115, 453
Lira P., 1996, MsT, 3
Maeda K., Taubenberger S., Sollerman J., Mazzali P. A., Leloudas G., Nomoto K., Motohara K., 2010, ApJ, 708, 1703
Maeda K., et al., 2011, MNRAS, 413, 3075
Maguire K., et al., 2012, MNRAS, 426, 2359
Marion G. H., Höflich P., Gerardy C. L., Vacca W. D., Wheeler J. C., Robinson E. L., 2009, AJ, 138, 727
Mandel K. S., Wood-Vasey W. M., Friedman A. S., Kirshner R. P., 2009, ApJ, 704, 629
Margutti R., Parrent J., Kamble A., Soderberg A. M., Foley R. J., Milisavljevic D., Drout M. R., Kirshner R., 2014, ApJ, 790, 52
Mazzali P. A., Chugai N., Turatto M., Lucy L. B., Danziger I. J., Cappellaro E., della Valle M., Benetti S., 1997, MNRAS, 284, 151
Mazzali P. A., Cappellaro E., Danziger I. J., Turatto M., Benetti S., 1998, ApJ, 499, L49
Mazzali P. A., Röpke F. K., Benetti S., Hillebrandt W., 2007, Sci, 315, 825
Matheson T., et al., 2012, ApJ, 754, 19
Meikle W. P. S., 2000, MNRAS, 314, 782
Nadyozhin D. K., 1994, ApJS, 92, 527
Nobili S., et al., 2005, A&A, 437, 789
Nobili S., Goobar A., 2008, A&A, 487, 19
Pastorello A., et al., 2007, MNRAS, 377, 1531
Peacock J. A., Schneider P., Efstathiou G., Ellis J. R., Leibundgut B., Lilly S. J., Mellier Y., 2006, ewg3.rept
Perlmutter S., et al., 1999, ApJ, 517, 565
Phillips M. M., 1993, ApJ, 413, L105
Phillips M. M., 2012, PASA, 29, 434
Phillips M. M., Lira P., Suntzeff N. B., Schommer R. A., Hamuy M., Maza J., 1999, AJ, 118, 1766
Phillips M. M., et al., 2006, AJ, 131, 2615
Phillips M. M., et al., 2013, ApJ, 779, 38
Pignata G., et al., 2008, MNRAS, 388, 971
Pinto P. A., Eastman R. G., 2000, ApJ, 530, 757
Riess A. G., Press W. H., Kirshner R. P., 1996, ApJ, 473, 88
Riess A. G., et al., 1998, AJ, 116, 1009
Scalzo R., et al., 2010, ApJ, 713, 1073
Scalzo R., et al., 2012, ApJ, 757, 12
Scalzo R., et al., 2014, MNRAS, 560
Stritzinger M., Leibundgut B., Walch S., Contardo G., 2006, A&A, 450, 241
Stritzinger M. D., et al., 2011, AJ, 142, 156
Suntzeff N. B., 1996, ssr..conf, 41
Tonry J. L., Dressler A., Blakeslee J. P., Ajhar E. A., Fletcher A. B., Luppino G. A., Metzger M. R., Moore C. B., 2001, ApJ, 546, 681
Tripp R., 1998, A&A, 331, 815
Tully R. B., 1988, ngc..book,
Valentini G., et al., 2003, ApJ, 595, 779
Weyant A., Wood-Vasey W. M., Allen L., Garnavich P. M., Jha S. W., Joyce R., Matheson T., 2014, ApJ, 784, 105
Wood-Vasey W. M., et al., 2008, ApJ, 689, 377

Acknowledgements. This research was supported by the DFG cluster of excellence Origin and Structure of the Universe' We would like to thank Chris Burns for his help with template fitting using SNooPy, Richard Scalzo for discussion on the nickel masses and Saraubh Jha on the nature of Type Ia supernovae. We thank Stephane Blondin for his comments on the manuscript. B.L. acknowledges support for this work by the Deutsche Forschungsgemeinschaft through TRR33, The Dark Universe and the Mount Stromlo Observatory for a Distinguished Visitorship during which most of this publication was prepared.